

Initiation of plate boundary slip in the Nankai Trough off the Muroto peninsula, southwest Japan

Takeshi Tsuji,¹ Toshifumi Matsuoka,² Yasuhiro Yamada,² Yasuyuki Nakamura,¹ Juichiro Ashi,¹ Hidekazu Tokuyama,¹ Shin'ichi Kuramoto,³ and Nathan L. Bangs⁴

Received 28 October 2004; revised 4 May 2005; accepted 18 May 2005; published 21 June 2005.

[1] To investigate variations in physical properties accompanying the development of the décollement, we used a neural network analysis of seismic attributes derived from 3D seismic reflection data gathered in the Nankai Trough convergent margin off the Muroto peninsula of southwest Japan. This analysis resulted in a detailed map of the geological features along the décollement and revealed a drastic change in physical properties at the sole of the proto-thrust. Ocean Drilling Program (ODP) data suggest that the décollement physical property change coincides with the initiation of slip. Furthermore, changes in the structure of the accretionary prism and reorganization of the décollement geometry also attend the initiation of plate boundary slip. **Citation:** Tsuji, T., T. Matsuoka, Y. Yamada, Y. Nakamura, J. Ashi, H. Tokuyama, S. Kuramoto, and N. L. Bangs (2005), Initiation of plate boundary slip in the Nankai Trough off the Muroto peninsula, southwest Japan, *Geophys. Res. Lett.*, 32, L12306, doi:10.1029/2004GL021861.

1. Introduction

[2] Many studies on the initiation and evolution of the décollement have been reported from various subduction zones [e.g., Moore *et al.*, 1998]. In the Nankai Trough off Muroto peninsula, the décollement has been well mapped beneath the accretionary prism on the seismic profile [Moore *et al.*, 1990], however it remains unknown what conditions control its development. To understand the development of the décollement, we need to investigate the physical properties (e.g. porosity and density) accompanying the development of the décollement. The development process also influences the frictional properties of the décollement. Therefore, the décollement plays a key role in accretionary prism growth. At the northern Barbados accretionary prism, porosity and density along the décollement were estimated using amplitude analyses of seismic reflection data [Shipley *et al.*, 1994]. Logging data and core samples from ten ODP sites within the Barbados 3D seismic survey area revealed the thickness and porosity of the décollement through direct measurement and seismic inversion [Bangs *et al.*, 1999; Zhao *et al.*, 2000]. In the case of the Nankai Trough, however, only two ODP sites (Site 808

and 1174) penetrate the décollement within the 3D seismic survey area [Moore *et al.*, 2001], thus an inversion approach is inappropriate. Furthermore, artifacts and other interference effects severely limit seismic reflection waveform analysis needed to map physical property variations. As an alternative, we estimate the physical properties along the Nankai Trough décollement via a neural network that considers multiple properties of the 3D seismic reflection data simultaneously [e.g., Strecker and Uden, 2002]. Similar methods have been used to characterize the physical properties of hydrocarbon reservoirs; our paper represents the first application of these techniques to a décollement.

2. Geologic Setting

[3] The Nankai Trough is the expression of the subduction of the Shikoku Basin section of the northern Philippine Sea plate under southwestern Japan (Figure 1). The rate of subduction is ~ 4 cm/yr along an azimuth of $310\text{--}315^\circ$ [Seno *et al.*, 1993]. The décollement in the Nankai Trough off the Muroto peninsula exists within a hemipelagic mudstone sequence at the deformation front [Taira *et al.*, 1991]. It is well defined by a prominent reverse-polarity reflector on seismic profiles (Figure 2). From this polarity reversal, the décollement is inferred to be a low acoustic impedance (velocity \times density) zone. The low acoustic impedance can be explained by high porosity sustained by high fluid pressure [Moore *et al.*, 1990]. This pore fluid pressure, far higher than hydrostatic, can account for the weak coupling along the décollement [e.g., Moore, 1989]. The prominent reverse-polarity décollement seismic reflection extends from beneath the accretionary prism to ~ 8 km seaward of the deformation front [Bangs *et al.*, 2004]. It spans across the transition from the active slip surface (the décollement proper) to the incipient slip surface (the “proto-décollement”) and into a horizon that has not yet slipped (the “future-décollement”). We cannot tell the amount of slip on these surfaces from the seismic data to properly define these segments. Therefore, we simply refer to the décollement as the portions where slip is certain (i.e. landward of the proto-thrust) and we refer to the décollement seismic reflection horizon (i.e. the décollement and its seaward extension) as “the décollement horizon.”

3. Three-Dimensional Seismic Reflection Data

[4] The 3D multi-channel seismic reflection data, acquired by the R/V Ewing in 1999 [Moore *et al.*, 2001], is analyzed for the purpose of investigating the geometry and physical properties of the décollement. The survey area is 80×8 km, comprising 81 individual lines with cross-track

¹Ocean Research Institute, The University of Tokyo, Tokyo, Japan.

²Graduate School of Engineering, Kyoto University, Kyoto, Japan.

³Center for Deep Earth Exploration, Japan Marine Science and Technology Center, Yokohama, Japan.

⁴Institute for Geophysics, University of Texas at Austin, Austin, Texas, USA.

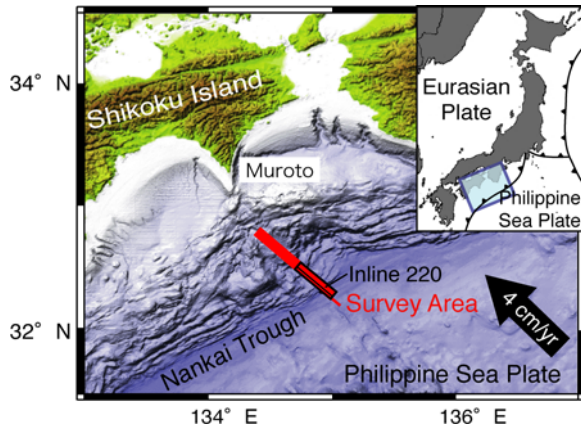


Figure 1. Bathymetric map of the Nankai Trough area. The red rectangle shows the 3D seismic reflection survey area. Our study area is the southern part of the survey area outlined with a black rectangle. The location of Inline 220, depicted in Figure 2, is shown as a black line.

spacing of 100 m (Figure 1). Due to streamer feathering by strong current, the total length of cross-line direction becomes 9 km. Processing included 3D pre-stack time migration and geometrical divergence correction. The data acquisition and processing details are described by *Bangs et al.* [2004].

[5] We focus on the formation of the décollement across a 33×9 km area at the southeastern end of the 3D seismic survey (Figure 2). The study area consists of three zones: the trench zone (TZ), the proto-thrust zone (PTZ), and the imbricate thrust zone (ITZ) [Moore et al., 2001]. The proto-thrust zone is characterized by one prominent thrust called the “proto-thrust”, the cut-off point of which corresponds to the deformation front at the seafloor (Figure 2). A region characterized by larger-scale thrust faulting is separated from the proto-thrust zone by a “frontal-thrust” and the wedge taper angle increases landward from the point where the frontal-thrust comes up to the seafloor.

[6] We reexamined the geometry of the décollement horizon and repicked it precisely on reverse-polarity phase of the décollement seismic reflection wavelet in order to determine physical property changes along this horizon (Figure 3a). Our observations reveal that the geometry of the décollement horizon seaward of the proto-thrust is not characterized by a continuous single surface but, rather, divides into two separate surfaces with a vertical offset of ~ 100 m (Figure 3b). These two horizons of the décollement converge into a single detachment surface immediately landward of the sole of the proto-thrust (Figure 2). This geometry suggests that the décollement may initially develop by merging or linking of originally separate fault planes, perhaps in a process analogous to the formation of a single slip surface from multiple fault splays [e.g., Reading, 1980].

4. Seismic Attributes Analysis via Kohonen Self-Organizing Map

[7] Seismic profiles generated using the seismic attributes enhance certain characteristic feature patterns which are unrecognizable on the original profile. However, it is

difficult to clearly identify the change in physical properties along the décollement horizon enhanced by each seismic attribute. Alternatively we consider seismic attributes in combination simultaneously in a neural network analysis, the output of which represents a clustering of the seismic volume into common patterns in seismic characteristics based on the selected attributes.

[8] We considered several seismic attributes that could be derived from the 3D seismic reflection data [e.g., *Taner et al.*, 1979]. The recorded seismic traces $f(t)$ can be thought of as a real part of the complex trace $F(t)$, which also has an imaginary part $g(t)$ that can be derived through the Hilbert transform.

$$F(t) = f(t) + i \cdot g(t) = A(t) \cdot e^{i\theta(t)}$$

The envelope $A(t)$, the reflection strength (A1), can be computed as a modulus of the complex trace. The instantaneous phase $\theta(t)$ (A2) is computed as the argument of the complex trace.

$$A(t) = \sqrt{f^2(t) + g^2(t)}$$

$$\theta(t) = \arctan(g(t)/f(t))$$

Since the envelope is independent of the phase, it directly represents the acoustic impedance contrasts. On the other hand, the instantaneous phase is independent of amplitude, thus it relates to the propagation phase of seismic wave front. The instantaneous frequency $freq(t)$ (A3) can then be computed as the time derivative of instantaneous phase and it represents the centroid of the power spectrum [Taner et al., 1979].

$$freq(t) = \frac{d\theta}{dt} = \frac{f(t) \cdot dg(t)/dt - df(t)/dt \cdot g(t)}{f^2(t) + g^2(t)}$$

An instantaneous quality factor $Q(t)$ (A4) can be computed with the following equation [Barnes, 1993].

$$Q(t) = -\pi \frac{freq(t)}{\sigma(t)}$$

$\sigma(t)$ is represented as time derivative of the envelope divided by the envelope. The lateral coherency of the

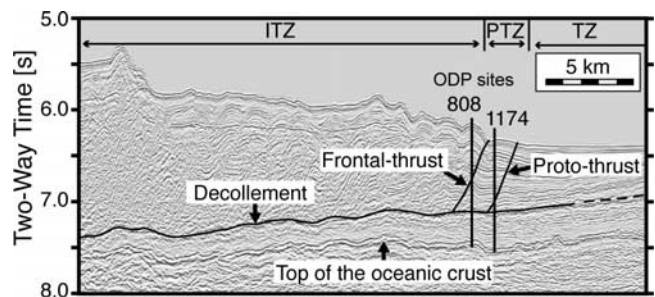


Figure 2. One of inline seismic profiles across the Nankai Trough, displayed with AGC. Vertical axis shows the two-way time in seconds (5.0–8.0 s).

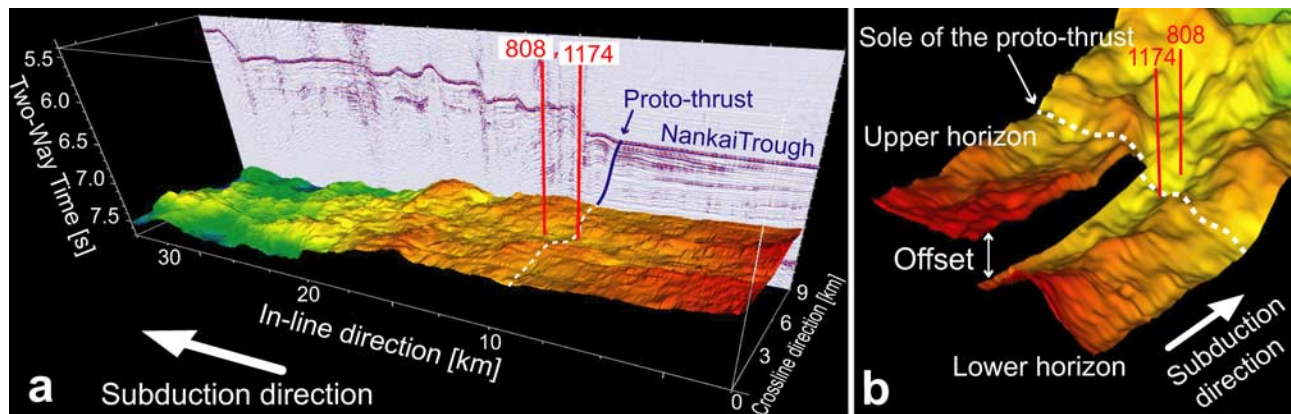


Figure 3. (a) Geometry of the décollement horizon acquired from 3D seismic reflection data. Vertical axis is two-way time in seconds (5.4–7.7 s). The horizon color is depth (two-way time) dependent. The white arrow shows the subduction direction of the Philippine Sea plate. Two red markers show the location of ODP Sites 1174 and 808. The white dashed line shows the classification boundary, corresponding to the sole of the proto-thrust. (b) The vertically exaggerated geometry of the décollement horizon around the sole of the proto-thrust. Note that, for comparison with Figure 3a, the angle of view is different.

seismic reflection (A5) was computed as semblance, because we are interested in the degree of the lateral variation of the décollement horizon.

[9] We used four seismic attributes, envelope (A1), instantaneous frequency (A3), instantaneous quality factor (A4), and semblance (A5), as input variables in a neural network system called the Kohonen self-organizing map (SOM) [Kohonen, 2001]. Although many different seismic attributes can be utilized, we considered these four sufficient to characterize the seismic waveform and associated properties. The SOM searches, recognizes, and classifies structural patterns in the four-dimensional vector that is constructed by the selected seismic attributes and spans the entire 3D seismic field [Strecker and Uden, 2002]. The output of the analysis classifies the seismic volume into several regions with common acoustic characteristics (represented by colors in Figure 4a). Previous experience has

shown that SOM is an effective tool for classifying seismic data into different features with geological significance [e.g., Strecker and Uden, 2002].

[10] We interpret the SOM classification along the décollement horizon (Figure 4a) to identify area with common physical properties. The SOM classification results show a clear boundary where the décollement intersects with the proto-thrust. The clarity of this boundary, together with the fact that other clear boundaries are not observed within our study area, implies that the physical properties along the décollement horizon change drastically at the sole of the proto-thrust.

[11] This classification result could be affected by seismic attenuation due to the thickening of the accretionary prism and the increase in seafloor roughness. To evaluate this influence, we calculated the power spectra of the reflections of Upper Shikoku Basin facies, located above

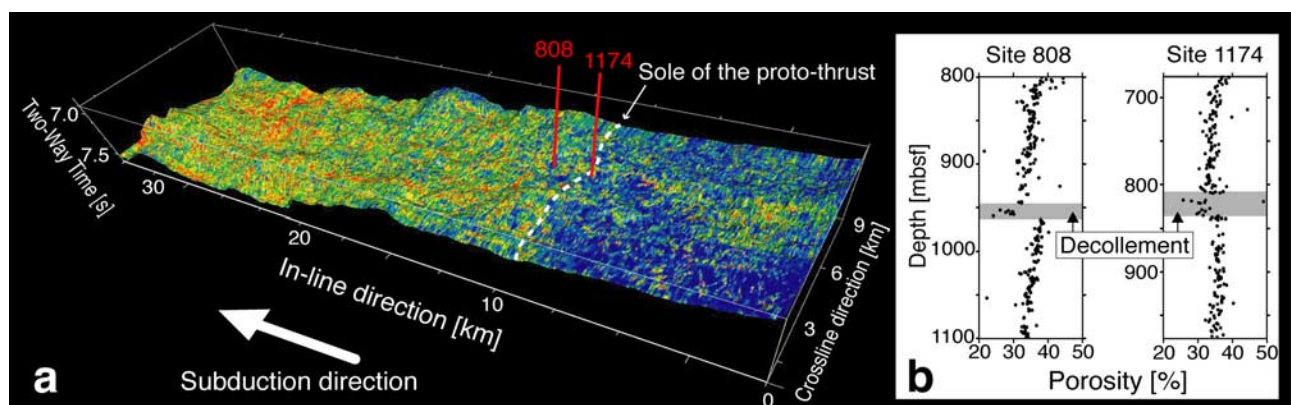


Figure 4. (a) Classification result along the décollement horizon by means of SOM. Vertical axis is two-way time in seconds (6.9–7.6 s). This figure is viewed from almost the same angle as Figure 3a. The regions with the same color belong to the same class and probably have similar physical properties. The white dashed line shows the classification boundary, which corresponds to the sole of the proto-thrust. (b) Comparison of the porosity measurement from Sites 1174 and 808. Black dots represent the porosity obtained from core samples. Vertical and horizontal axes represent the depth and the porosity, respectively. Shaded zone shows the position of the décollement.

the décollement. These power spectra do not change abruptly above the SOM classification boundary, thus the influence of such attenuation on our SOM classification results is minimal.

5. Interpretation

[12] ODP Sites 1174 and 808 [Moore *et al.*, 2001] are located within our study area. Site 1174 penetrates the proto-thrust and intersects the décollement just seaward of the SOM classification boundary described above (Figure 4a). Site 808 is located 1.7 km landward of the proto-thrust and on the landward side of the SOM classification boundary. At Site 1174, the porosity of the décollement measured from core samples changes little across the décollement by comparison to Site 808, where porosity increases from $\sim 30\%$ above the décollement to $\sim 40\%$ below it (Figure 4b). Furthermore, the fault zone thins from ~ 32 m to ~ 18 m between Sites 1174 and 808 respectively. The difference between porosity patterns of two sites indicates the development of the décollement zone from Site 1174 to Site 808 [Screaton *et al.*, 2002].

[13] We infer that the décollement between the two ODP sites developed following release of shear stress through slip along the décollement and the proto-thrust. The proto-thrust is the most seaward thrust and therefore slip along the décollement virtually terminates at the intersection with the proto-thrust. The release of shear stress from slip causes a highly brecciated and a narrowly focused fault zone to develop as observed in the porosity profile of Site 808 (Figure 4b). The selected seismic attributes for the SOM classification are affected greatly by porosity, consequently the SOM classification (Figure 4a) varies with changes in décollement horizon physical properties. Therefore, our classification result indicates that the décollement developed rapidly rather than gradually between Site 1174 and Site 808 (at the sole of the proto-thrust).

[14] Furthermore, our SOM classification boundary (Figure 4a) is in good agreement with the convergence point of the two separated décollement horizons (Figure 3b). This geometry may be kinematically controlled by the frictional coefficient along the décollement horizon. Conditions conducive for décollement initiation could potentially develop in several stratigraphic horizons below the low permeability sequences that lie beneath the rapidly deposited trench turbidites. It is therefore not surprising that two décollement horizons are seen to comprise the incipient décollement where slip is still negligible. As displacement increases, however, these two horizons may merge into a single detachment surface to decrease the frictional coefficient; the morphology of the décollement horizon itself may reflect this process of coalescing disparate slip surfaces to accommodate increased displacement. The geometry of the décollement, thus, supports our interpretation of the SOM classification results.

[15] Seismic profiles image the tectonic thickening of the accretionary prism that has occurred following displacement along the frontal-thrust (Figure 2). The thickened prism increases the overburden load on the décollement horizon, landward of the frontal-thrust intersection with the seafloor and coincident with our SOM classification boundary

(Figure 4a). This increase of vertical load and a low permeability cap [Brown *et al.*, 1994; Ujiie *et al.*, 2003] may raise the fluid pressure along the décollement horizon. Furthermore, there is a possibility of clay dehydration, which raises the fluid pressure at the décollement horizon, especially near the deformation front [Steurer and Underwood, 2003]. According to Mohr-Coulomb theory, the high fluid pressure reduces the shear strength along the décollement horizon because effective normal stress decreases, thus allowing slip to occur more easily in the landward class region. The slip in the seaward class region is, however, negligible owing to a higher frictional coefficient under lower fluid pressure. Thus, the SOM classification results reveal the boundary between the décollement where active slip occur and the incipient décollement where displacement is negligible.

6. Summary and Conclusions

[16] Seismic attributes analysis via SOM was applied to delineate physical properties along the Nankai Trough décollement horizon. The SOM classification result clearly shows a change in physical properties at the intersection of the décollement and the proto-thrust. The SOM classification result, coupled with analysis of the structure of the accretionary prism and the geometry of the décollement horizon, indicates the décollement organizes itself into a single coherent slip surface at the sole of the proto-thrust, which then abruptly alters the décollement physical properties. We therefore conclude that the active slip of the décollement proper initiates at the sole of the proto-thrust.

[17] **Acknowledgments.** We are grateful to M. Coffin and D. Curewitz, G. Iturrino, and T. Ulrych for the helpful comments, and T. Shipley, S. Gulick, and G. Moore for seismic data. We also thank T. Taner (Rock Solid Images) for the neural network tool.

References

- Bangs, N. L., T. H. Shipley, J. C. Moore, and G. F. Moore (1999), Fluid accumulation and channeling along the northern Barbados Ridge décollement thrust, *J. Geophys. Res.*, *104*, 20,399–20,414.
- Bangs, N. L., T. Shipley, S. Gulick, G. Moore, S. Kuramoto, and Y. Nakamura (2004), Evolution of the Nankai Trough décollement from the trench into the seismogenic zone: Inferences from three-dimensional seismic reflection imaging, *Geology*, *32*, 273–276.
- Barnes, A. E. (1993), Instantaneous spectral bandwidth and dominant frequency with applications to seismic data, *Geophysics*, *58*, 419–428.
- Brown, K. M., B. Bekins, B. Clennell, D. Dewhurst, and G. Westbrook (1994), Heterogeneous hydrofracture development and accretionary fault dynamics, *Geology*, *22*, 259–262.
- Kohonen, T. (2001), *Self-Organization Maps*, 3rd ed., Springer, New York.
- Moore, G. F., T. H. Shipley, P. L. Stoffa, D. E. Karig, A. Taira, S. Kuramoto, H. Tokuyama, and K. Suyehiro (1990), Structure of the Nankai Trough accretionary zone from multichannel seismic reflection data, *J. Geophys. Res.*, *95*, 8753–8765.
- Moore, G. F., et al. (2001), *Proceedings of the Ocean Drilling Program, Initial Reports*, 190 [CD-ROM], Ocean Drill. Program, College Station, Tex.
- Moore, J. C. (1989), Tectonics and hydrogeology of accretionary prisms: Role of the décollement zone, *J. Struct. Geol.*, *11*, 95–106.
- Moore, J. C., et al. (1998), Consolidation patterns during initiation and evolution of a plate-boundary décollement zone: Northern Barbados accretionary prism, *Geology*, *26*, 811–814.
- Reading, H. G. (1980), Characteristics and recognition of strike-slip fault systems, in *Sedimentation in Oblique-Slip Mobile Zones*, edited by P. E. Balance and H. G. Reading, *Spec. Publ. of the Int. Assoc. of Sedimentol.*, *4*, 7–26.

- Screaton, E., D. Saffer, P. Henry, S. Hunze, and Leg 190 Shipboard Scientific Party (2002), Porosity loss within the underthrust sediments of the Nankai accretionary complex: Implications for overpressures, *Geology*, *30*, 19–22.
- Seno, T., S. Stein, and A. E. Gripp (1993), A model for the motion of the Philippine Sea plate consistent with NUVEL-1 and geological data, *J. Geophys. Res.*, *98*, 17,941–17,948.
- Shipley, T. H., G. F. Moore, N. L. Bangs, J. C. Moore, and P. L. Stoffa (1994), Seismically inferred dilatancy distribution, northern Barbados Ridge décollement: Implications for fluid migration and fault strength, *Geology*, *22*, 411–414.
- Steurer, J. F., and M. B. Underwood (2003), Clay mineralogy of mudstones from the Nankai Trough reference site 1172 and 1177 and frontal accretionary prism site 1174, *Proc. Ocean Drill. Program Sci. Results*, *190/196*, 1–37.
- Strecker, U., and R. Uden (2002), Data mining of 3D poststack seismic attribute volumes using Kohonen self-organizing maps, *Leading Edge*, *10*, 1032–1037.
- Taira, A., et al. (1991), *Proceedings of the Ocean Drilling Program, Initial Reports*, 131, Ocean Drill. Program, College Station, Tex.
- Taner, M. T., F. Koehler, and R. E. Sheriff (1979), Complex seismic traces analysis, *Geophysics*, *44*, 1041–1063.
- Ujiie, K., T. Hisamitsu, and A. Taira (2003), Deformation and fluid pressure variation during initiation and evolution of the plate boundary décollement zone in the Nankai accretionary prism, *J. Geophys. Res.*, *108*(B8), 2398, doi:10.1029/2002JB002314.
- Zhao, Z., G. F. Moore, N. L. Bangs, and T. H. Shipley (2000), Spatial variations of the décollement/protodécollement zone and their implications: A 3D seismic inversion study of the northern Barbados accretionary prism, *Island Arc*, *9*, 219–236.

J. Ashi, Y. Nakamura, H. Tokuyama, and T. Tsuji, Ocean Research Institute, University of Tokyo, 1-15-1 Minamidai, Nakano-ku, Tokyo 164-8639, Japan. (tsuji@ori.u-tokyo.ac.jp)

N. L. Bangs, University of Texas at Austin, Institute for Geophysics, 4412 Spicewood Springs Rd., Austin, TX 78759, USA.

S. Kuramoto, Center for Deep Earth Exploration, Japan Marine Science and Technology Center, 2-15 Natsushima-cho, Yokosuka, Kanagawa 237-0061, Japan.

T. Matsuoka and Y. Yamada, Graduate School of Engineering, Kyoto University, Yoshida hon-machi, Sakyo-ku, Kyoto 606-8501, Japan.